INTERFACE

royalsocietypublishing.org/journal/rsif

Research

Cite this article: Volkov AG, Xu KG, Kolobov VI. 2019 Plasma-generated reactive oxygen and nitrogen species can lead to closure, locking and constriction of the *Dionaea muscipula* Ellis trap. *J. R. Soc. Interface* **16**: 20180713.
http://dx.doi.org/10.1098/rsif.2018.0713

Received: 23 September 2018
Accepted: 30 November 2018

Subject Category:
Life Sciences–Chemistry interface

Subject Areas:
biophysics, biochemistry, biomechanics

Keywords:
action potential, *Dionaea muscipula* Ellis, ion channels, plasma, reactive oxygen and nitrogen species, Venus flytrap

Author for correspondence:
Alexander G. Volkov
e-mail: agvolkov@yahoo.com

THE ROYAL SOCIETY
PUBLISHING

Plasma-generated reactive oxygen and nitrogen species can lead to closure, locking and constriction of the *Dionaea muscipula* Ellis trap

Alexander G. Volkov[1], Kunning G. Xu[2] and Vladimir I. Kolobov[3,4]

[1]Department of Chemistry and Biochemistry, Oakwood University, Huntsville, AL 35896, USA
[2]Mechanical and Aerospace Engineering Department, and [3]The Center for Space Plasma and Aeronomic Research, The University of Alabama in Huntsville, Huntsville, AL 35899, USA
[4]CFD Research Corporation, Huntsville, AL 35806, USA

AGV, 0000-0002-6292-612X

Reactive oxygen and nitrogen species (RONS) can influence plant signalling, physiology and development. We have previously observed that an argon plasma jet in atmospheric air can activate plant movements and morphing structures in the Venus flytrap and *Mimosa pudica* similar to stimulation of their mechanosensors *in vivo*. In this paper, we found that the Venus flytrap can be activated by plasma jets without direct contact of plasma with the lobe, midrib or cilia. The observed effects are attributed to RONS, which are generated by argon and helium plasma jets in atmospheric air. We also found that application of H_2O_2 or HNO_3 aqueous solutions to the midrib induces propagation of action potentials and trap closing similar to plasma effects. Control experiments showed that UV light or neutral gas flow did not induce morphing or closing of the trap. The trap closing by plasma is thus likely to be associated with the production of hydrogen peroxide by the cold plasma jet in air. Understanding plasma control of plant morphing could help design adaptive structures and bioinspired intelligent materials.

1. Introduction

Plasma is a Greek word which has different meanings in physics, medicine, biology and geology. In medicine, plasma is the colourless fluid which remains after removal of cells from blood, lymph or milk. In biology, a plasma membrane denotes a cell membrane that forms an external boundary of the cytoplasm of a cell or encloses a vacuole. In geology, plasma is a dark green, translucent variety of quartz.

In physics, plasma denotes a quasi-neutral ionized gas. In 1922, Irving Langmuir proposed that the electrons, ions and neutrals in an ionized gas could be considered as corpuscular material entrained in some kind of fluid medium. Langmuir called this entraining medium plasma because it reminded him of blood plasma. In reality, however, there is no 'fluid medium' that entrains the electrons, ions and neutrals. Instead, electric fields produced in plasma to maintain its quasi-neutrality hold together electrons and ions. As our present paper is at the interface of physics and plant biology, we first want to clarify that this work deals with ionized gas plasma, not biological plasma.

Most of the substances in the Universe are in the form of plasma. On Earth, plasma is generated naturally in lightning and the aurora borealis. Since the beginning of the twentieth century, the observed effects of the aurora borealis on plants and trees have been associated with ions generated by atmospheric electricity near the Earth's surface. During his visits to the Arctic, Karl Lemström was surprised how green and healthy the vegetation looked and wondered whether this might be due to the air ions carried through the

© 2019 The Author(s) Published by the Royal Society. All rights reserved.

atmosphere from the aurora borealis. The related research was termed 'electroculture' [1,2].

In the laboratory, plasma is often produced in vacuum chambers at low gas pressure and is widely used for semiconductor fabrication and material processing. Plasma-aided manufacturing is an enabling technology for micro- and nano-electronics. At the end of the twentieth century, it was found that plasma can also be created in small volumes in atmospheric-pressure air at room temperature. This low-temperature plasma (LTP), also called cold plasma, has found an increasing number of applications in medicine for disinfection and sterilization, dermatology, dentistry, oncology, etc. The associated field is termed 'plasma medicine'.

Over the last decade, it was found that cold plasma may also be beneficial for improving seed germination, disinfection of seeds, protection from bacterial infection, acceleration of plant growth and food processing. The associated field is termed 'plasma agriculture' [3].

Often termed the fourth state of matter, plasma is formed when electricity passes through gas (the third state of matter). Gas ionization by electrons provides a unique catalytic environment for a variety of chemical reactions at ambient gas temperatures. Interactions of LTP with biological matter and their potential applications are currently a topic of significant interest [4–7]. The observed effects of plasma on biological cells are believed to be mediated by plasma-produced reactive oxygen species (ROS) and reactive nitrogen species [8]. Among these are hydroxyl (OH), atomic oxygen (O), singlet delta oxygen ($O_2(1D)$), superoxide (O_2^-), hydrogen peroxide (H_2O_2) and nitric oxide (NO). These species can interact with cell membranes, enter the cell and increase the intracellular ROS concentrations, which may lead to DNA damage and may compromise the integrity of other organelles and macromolecules. Reactive oxygen and nitrogen species (RONS) can also trigger cell signalling cascades, which can ultimately lead to cellular death pathways, such as apoptosis, in addition to triggering beneficial immune responses. ROS are beneficial to plants, and maintaining a basal level of ROS in cells is essential for life [9].

Several cold plasma sources have been approved for wound healing, dentistry and cancer treatment. To fully realize their potential in any biomedical application, a full characterization of the plasma sources with respect to controlled RONS generation and transport is needed. Some of the species, such as atomic oxygen and nitrogen (O and N), ozone (O_3), excited states of molecular oxygen (e.g. $O_2(1D)$) or nitric oxides, have previously been quantified experimentally and computationally in oxygen- and nitrogen-containing plasmas. Computational modelling has also provided insight into the plasma delivery of RONS into liquids and tissue [10,11]. These simulations determined that plasma can deliver ozone (O_3), H_2O_2 and nitrogen oxides (NO_x) to tissue covered with a thin liquid layer. In biofilms, H_2O_2 and molecular oxygen (O_2) can penetrate up to millimetre depths.

The nature of cold plasma interactions with plants is the subject of active research [12]. We have previously observed that an argon plasma jet in atmospheric air can activate plant movements and morphing structures in Venus flytrap and *Mimosa pudica* similar to stimulation of their mechanosensors *in vivo* [13]. However, there was no explanation of the observed effects.

Cold plasmas have four main components that can affect plants: charged particles (ions and electrons), photons (including UV light), electromagnetic fields and reactive neutral species such as RONS [13]. Some of the RONS are known to play important roles in plant physiology. They can be very toxic to biological tissue, mitochondria, bacteria, fungi and viruses. At the same time, RONS are beneficial to developmental processes of plants and activation of ion channels [14]. In our new experiments, we have observed that the morphing effects occur without direct contact of the plant surface with the cold plasma jet, which indicates that the plasma-produced RONS may be the main cause of the observed effects.

In the present paper, we report detailed observations of the cold plasma effects on the Venus flytrap morphing structures using helium and argon plasma jets in atmospheric air. Venus flytrap (*Dionaea muscipula* Ellis) is a marvellous plant that has intrigued scientists since the times of Charles Darwin [15]. It is the most famous among carnivorous plants, which can attract and quickly capture insects. The traps of the Venus flytrap have mechanosensing hairs that can receive, process and transfer information about an insect's mechanical stimuli. Touching the trigger hairs, which protrude from the upper leaf epidermis of the Venus flytrap, activates mechanosensitive ion channels and generates receptor potentials [16], which can induce action potentials [17]. It was found that two action potentials are required to trigger the trap closing [17,18].

The mechanism of the fast trap movement and morphing has been debated for a long time [19–23]. In the most recent hydroelastic curvature model, the upper leaf of the Venus fly trap is visualized as a thin, weakly curved elastic shell with principal natural curvatures that depend on the hydrostatic state of the two surface layers of the cell, where different hydrostatic pressures are maintained [22]. Unequal expansion of individual layers results in bending of the leaf, which is described in terms of bending elasticity. External triggers, mechanical, electrical, plasma or infrared laser result in the opening of pores connecting these layers; water then runs from one layer to another layer within a lobe, and the lobe quickly changes its curvature from convex to concave, and the trap closes. Equations describing this movement were derived and verified with experimental data [22]. The entire hunting cycle from catching the fly to tightening, digesting and reopening the trap was described by Volkov *et al*. [24,25].

2. Material and methods

Two hundred bulbs of *D. muscipula* (Venus flytrap) were purchased for this experimental work from Fly-Trap Farm (Supply, NC, USA). All plants were cultivated from seeds. The soil was treated with distilled water. All plants were grown in well-drained pots at 22°C with a 12 : 12 h light : dark photoperiod. The irradiance was 900–1000 µmol photons m^{-2} s^{-1} photosynthetically active radiation at plant level. The plants were watered by distilled water. The humidity averaged 45–50%. All experiments were performed on different healthy adult specimens. We did not use the same trap twice.

Hydrogen peroxide solution and HNO_3 were purchased from Sigma-Aldrich (USA). $HgCl_2$, KCl, $CaCl_2$ and tetraethylammonium chloride (TEACl) were obtained from Fluka (New York, NY, USA).

All measurements were conducted in the laboratory at 21°C inside a Faraday cage mounted on a vibration-stabilized table. Teflon-coated silver wires (A-M Systems, Inc., Sequim, WA, USA) with a diameter of 0.2 mm were used for preparation of

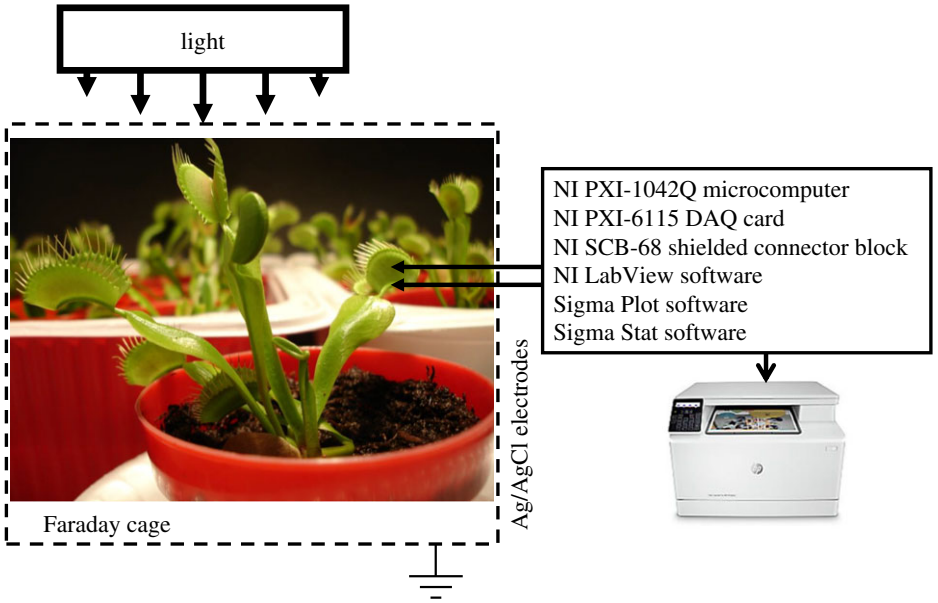

Figure 1. Diagram of experimental set-up for electrophysiological experiments. Ag/AgCl electrodes were used for measurements of plant electrical responses. (Online version in colour.)

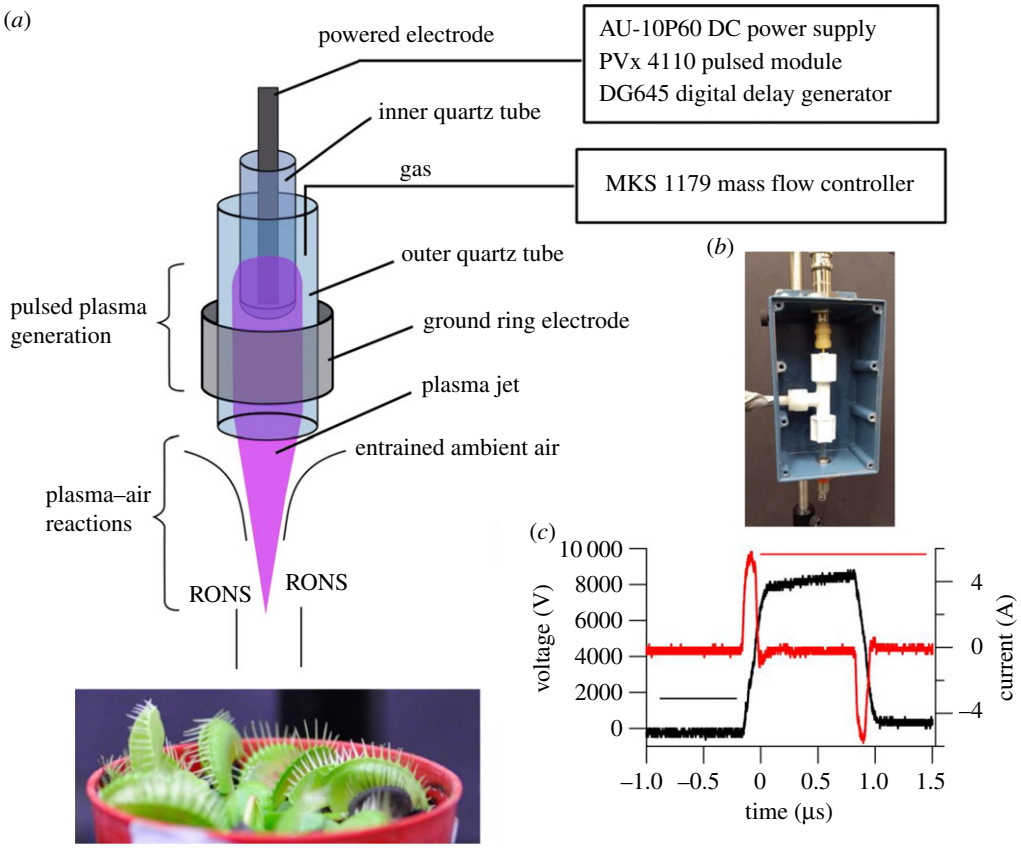

Figure 2. Schematic diagram of the cold plasma jet interacting with a Venus flytrap (*a*). The device with the shielding cover off (*b*). Typical voltage and current waveform for one pulse (*c*).

non-polarizable electrodes. Reversible Ag/AgCl electrodes were prepared in the dark by electrodeposition of AgCl on 5 mm long silver wire tips without Teflon coating in a 0.1 M KCl aqueous solution. The anode was a high-purity silver wire and the cathode was a platinum plate. Electrical current in the electrolytic cell was limited to 1 mA of the anode's surface. Stabilization of electrodes was accomplished by placing two Ag/AgCl electrodes in a 0.1 M KCl solution for 24 h and connecting a short circuit between them. The response time of Ag/AgCl electrodes was less than 0.1 µs. Identical Ag/AgCl electrodes were used as working and reference electrodes for measurements of potential differences in the plants. Following insertion of the electrodes into lobes and a midrib, the traps closed. We allowed plants to rest until the traps were completely open again.

The experimental set-up for data acquisition is shown in figure 1. Three different data acquisition systems were used in the present work. High-speed data acquisition was performed using microcomputers with a simultaneous multifunction I/O plug-in data acquisition board NI-PXI-6115 (National Instruments, Austin, TX, USA) interfaced through a NI SCB-68

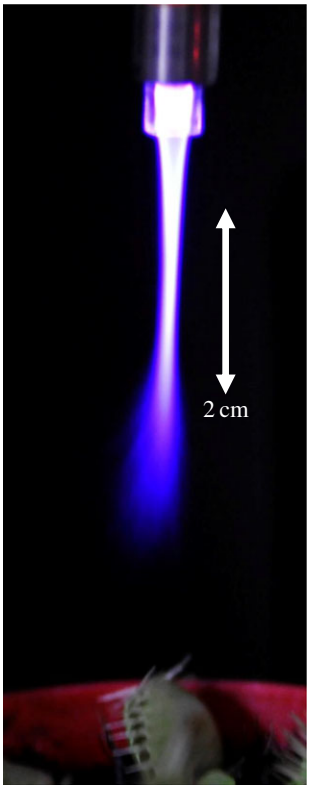

Figure 3. Light emission from helium plasma jet injected in atmospheric air and its activation of the Venus flytrap morphing.

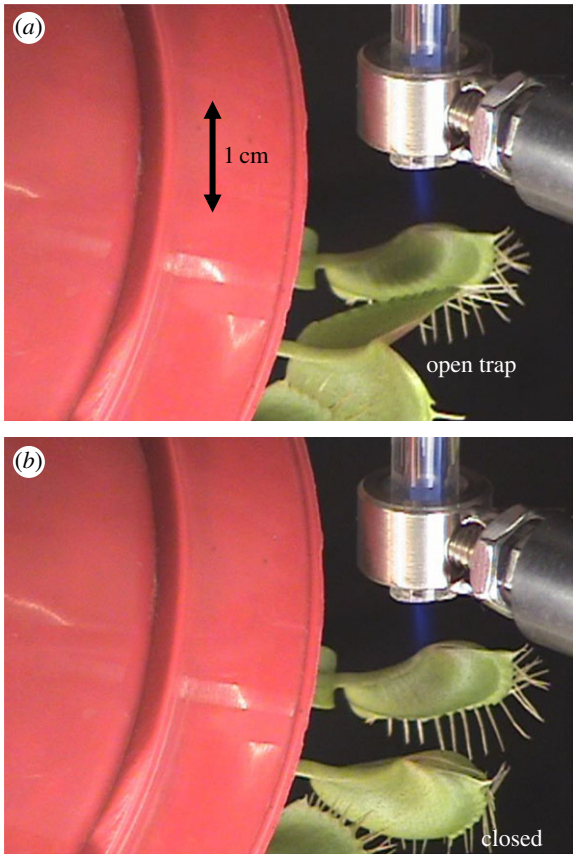

Figure 4. Closing of the trap (*a*) by argon plasma activation of the external surface of a lobe (*b*). (Online version in colour.)

shielded connector block to Ag/AgCl electrodes. The system integrates standard low-pass anti-aliasing filters at one-half of the sampling frequency. The data acquisition board NI-PXI-6115 (National Instruments, Austin, TX, USA) has a maximum sampling rate of 4 000 000 samples s^{-1}.

Digital video recorders, Sony DCR-HC36 and HD AVCHD, were used to monitor the Venus flytraps and to collect digital images, which were analysed frame by frame using Sony Vegas 13 software. A Nikon D3x camera with an AF-S Micro Nikkor 105 mm 1 : 2.8 G ED VR lens (Nikon, USA) was used to photograph the Venus flytrap.

Software SigmaPlot 12 (Systat Software, Inc.) was used for statistical analysis of the experimental data. All experimental results were reproduced at least 25 times using different plants.

The cold plasma jets used in our experiments have an annular geometry with two nested quartz tubes (figure 2*a*). The working gas flows between the tubes in the annulus. The outer tube has an outer diameter of 6 mm and inner diameter of 4 mm and is open at both ends. The inner tube has an outer diameter of 3 mm and an inner diameter of 2 mm and is closed at one end. The tubes are held inside a standard plastic compression Tee tube fitting (Swagelok NY-400-3) with the gas line at the perpendicular leg of the tee. This creates a sealed volume with the only outlet being the annular space between the quartz tubes.

The entire plasma jet source was placed in a metal enclosure with a few centimetres of the tube extending outside of the enclosure (figure 2*b*). A 1 mm diameter tungsten pin was inserted into the inner tube. A high-voltage coaxial power connector provided shielded power delivery. The central pin carries the high-voltage signal from the pulsed DC power source to the tungsten pin. The grounded shield of the coaxial connector was connected to the metal enclosure, which acts as the second grounded electrode. This design prevents direct contact between the plasma in the annulus and either electrode, thus preventing arcing, which would damage the plants.

The pulsed DC power source was driven at 9 kV, 16 mA, 6 kHz frequency and 1 µs pulsed width (figure 2*c*). The power source consisted of a Matsusada AU-10P60 10 kV DC power supply, an IXYS PVX-4110 pulsed generator and an SRS DG-645 delay generator. The pulse had a square shape with a slight slope during the rising edge. The current trace had two distinct current pulses at the rising and failing fronts of the voltage (figure 2*c*). Bottled helium, argon and air from an air compressor were metered with MKS digital mass flow controllers. The helium flow rate was set at 2.9 l min^{-1} and air was added at 0.149 l min^{-1}, approximately 5% air by volume. The plasma jet with pure helium was approximately 4 cm long. With air added, the jet length shrank to 2 cm. Argon flowed at a rate of 1.55 l min^{-1} between the two tubes. The gas was ionized by the strong electric field between the electrodes, and formed a plasma jet approximately 2–4 cm long, as measured from the exit of the outer tube, depending on the gas mixture.

Although the plasma jet looks continuous to the naked eye or to a low-speed camera as seen in figure 3, it actually consists of fast ionization waves (plasma bullets) propagating along the noble gas channel with speeds of approximately a few hundred metres per second. Electrons inside the fast ionization wave have energies of a few electron volts and are capable of producing ionization and non-equilibrium chemical reactions at room temperature. The reactive species in the noble gas–air mixture were generated by these electrons in the areas where mixing of the noble gas with air takes place. The charged species (electrons and ions) recombine quickly beyond the plume (the glow plasma region), but the neutral species with longer life times can propagate beyond the plasma plume and interact with plants. The extent of the charged species presence was not explicitly measured here, but some comparisons can be made with other similar works in the literature. Van Gessel *et al*. [26] measured the electron density in a cold plasma jet using laser-induced scattering and showed that the density decreased by an order of magnitude from the tube exit to 6 mm downstream. Xu and

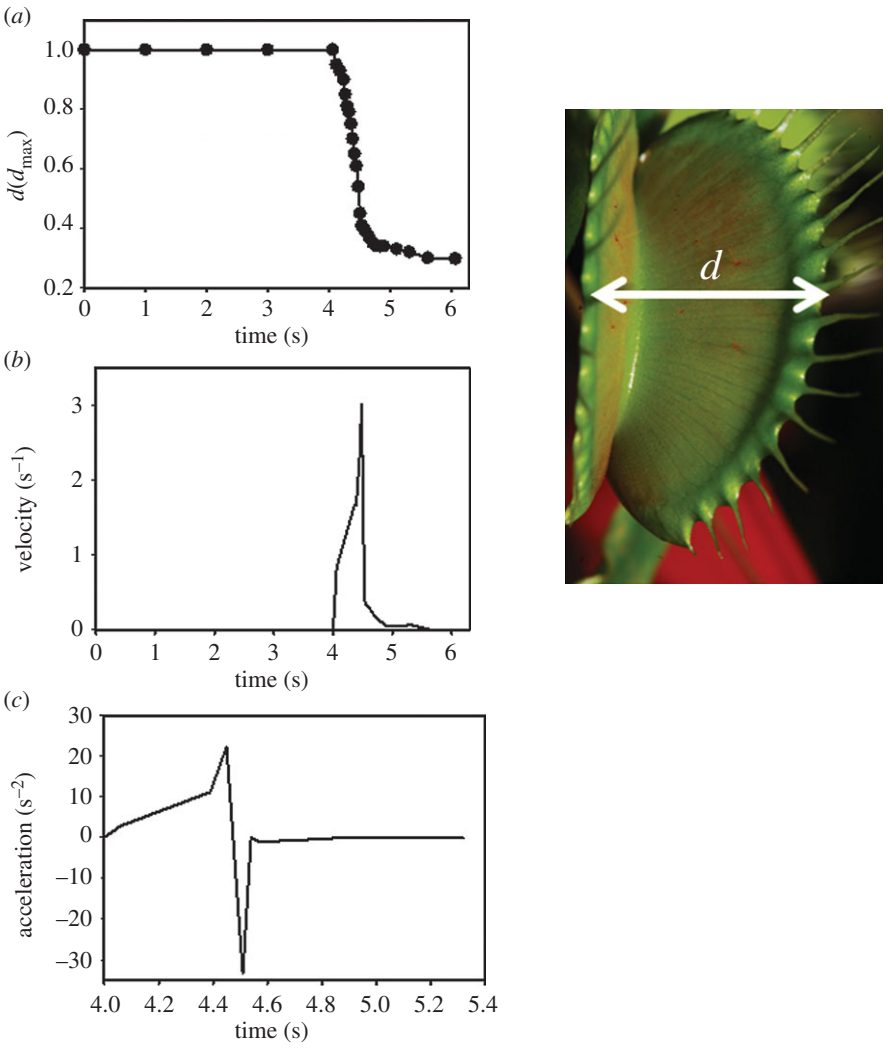

Figure 5. The distance (*a*), velocity (*b*) and acceleration (*c*) of the trap closing by low-temperature plasma stimulation of cilia of the Venus flytrap. (Online version in colour.)

Doyle [27] measured the electron density in a radiofrequency (RF) atmospheric plasma jet with Langmuir probes and found the density decreased from one to three orders of magnitude approximately 7 mm downstream of the exit. It is important to point out that direct comparison between different atmospheric plasma jets is difficult as geometry, power and gas flow and composition cause significant differences in the resulting plasma properties.

3. Results

3.1. Trap morphing by plasma

Figure 3 shows light emission from a helium plasma jet in atmospheric air. Two types of glow regions can be clearly distinguished: a bright white core region, which corresponds to the helium plasma, and a blue outer region, which corresponds to the mixed He–air plasmas. In the blue region, gas mixing and generation of RONS take place. These RONS propagate beyond the plasma region owing to gas convection and diffusion. There is a wide gap between the plasma glow and the plant position to eliminate charged particles or direct plasma contact as the cause of trap closure.

The plasma jet had a maximum spot size of 3 mm diameter based on the inner diameter of the outer quartz tube. The spot size decreased with axial distance until the jet disappeared. The plasma-generated species such as RONS remained within a small cylinder around the jet as they were formed from entrained air. Thus the exposed area was estimated to be less than 5 mm in diameter. Furthermore, only a small part of the Venus flytrap tissue, such as a lobe, the midrib or cilia, was exposed to plasma-derived species. Only one plasma-treated trap can be closed at a time. Other traps from the same plant need separate treatment for plasma-activated closing.

Applying an atmospheric pressure He or Ar plasma jet to the inside or outside of a lobe, midrib or cilia in *D. muscipula* Ellis induces trap morphing and closing (figure 4). Additional application of plasma to an already closed trap induces closed trap locking, tightening and its transition from convex to concave morphing structures just like stimulation of the mechanosensors or trigger hairs *in vivo*. Using video recording, it is possible to estimate the speed and acceleration of lobe rims during trap closing. The dynamics of lobe movement induced by application of a plasma jet to cilia or to the internal surface of the midrib of the Venus flytrap is shown in figures 5 and 6. Stimulation of a midrib or lobes (figure 6) by cold plasma induces fast closing of a trap with speeds up to 16 cm s^{-1} and accelerations up to 800 cm s^{-12}, similar to mechanical stimulation of trigger hairs [22,24,25]. Plasma stimulation of cilia (figure 5) induces closing of a trap with slow speed and acceleration. Gentle mechanical

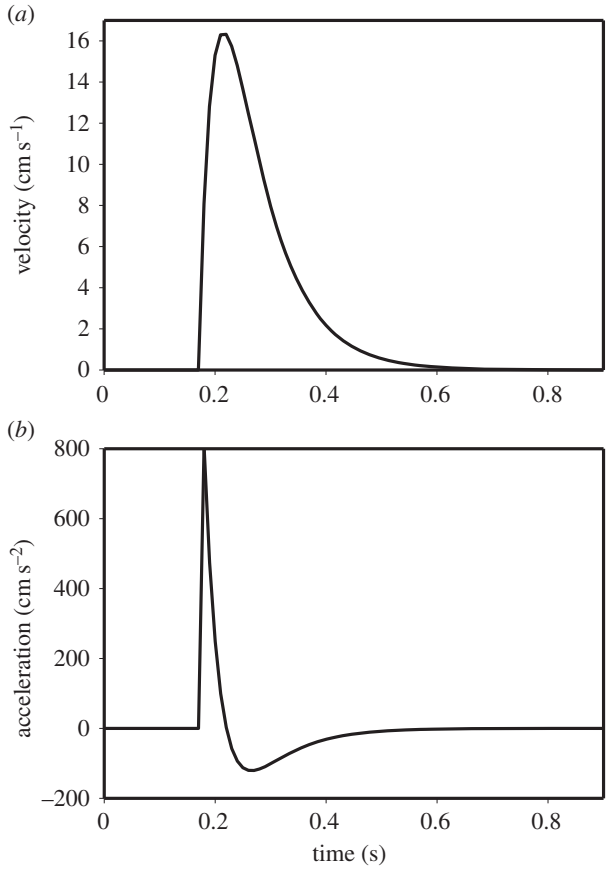

Figure 6. Velocity (*a*) and acceleration (*b*) of the trap closing by low-temperature plasma stimulation of the Venus flytrap's midrib. Solid lines are estimated from equation (4.2).

stimulation of cilia does not induce morphing and closing of traps. The plasma jet can close the trap without directly touching the upper leaf with an air gap of about 1 cm between the tip of the plasma jet and the trap surface, which is approximately 5 cm from the tube exit.

Plasma treatment of a petiole for 20–40 s did not induce any movements in the Venus flytrap. Application of cold plasma with direct contact of the plume with the plant tissue for a short period of time to any point in the Venus flytrap did not cause any injury or damage and is deemed safe for plants. The trap closed by cold plasma reopened completely within 2 days of the transition from the concave to convex shape.

3.2. Comparison of trap morphing by liquid reactive oxygen and nitrogen species

Venus flytrap morphing and trap closing could be caused by the generation of RONS by plasma. It is well known that H_2O_2 activates plasma membrane Ca^{2+}-permeable channels in *Arabidopsis* inhibits inward K^+ channel activity, but does not promote the activity of outward K^+ channels [14,28]. Figure 7*a* shows that applying just 10 µl of 3% H_2O_2 or 10 mM HNO_3 aqueous solution (figure 7*b*) to the midrib closes the trap (mean 76%, median 100%, s.d. 43.6%, s.e. 8.72%, 95% CI 18%, 99% CI 24.4%, $n = 25$ for H_2O_2 and mean 93.1%, median 100%, s.d. 25.8%, s.e. 4.79%, 95% CI 9.8%, 99% CI 13.2%, $n = 29$ for HNO_3), similar to the effects of plasma. Applying 10 µl of water to the midrib does not close the trap. RONS produced by cold plasma appear to be the primary reason for plasma-induced chemotropic activation

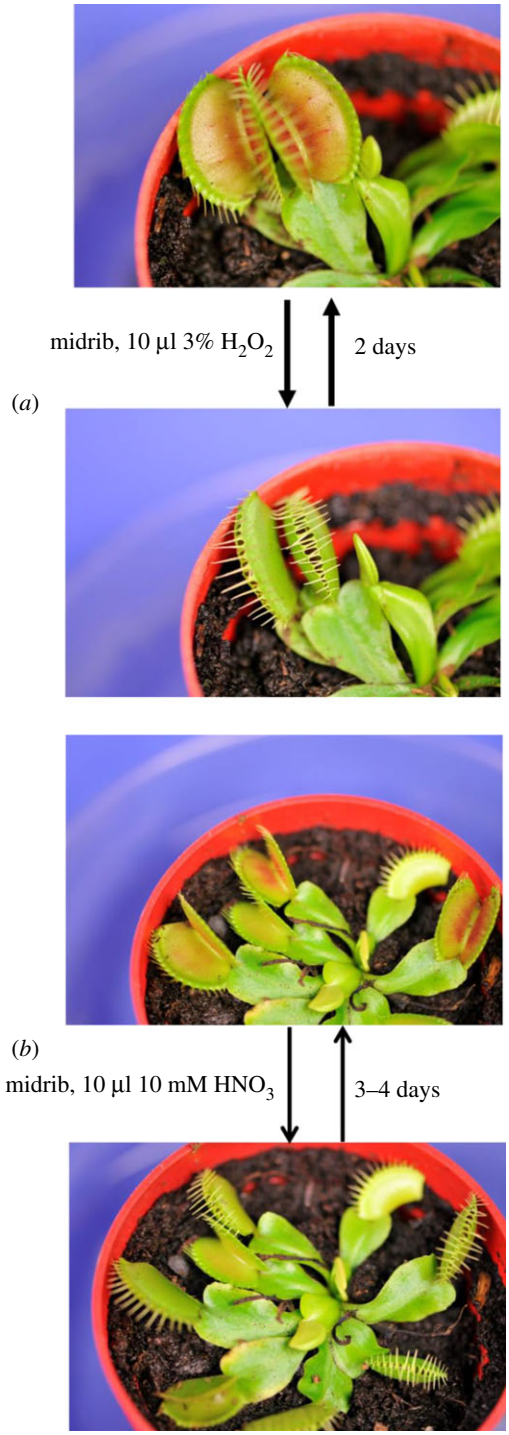

Figure 7. Closing and opening of a trap by deposition of 10 µl drops of 3% H_2O_2 (*a*) or 0.01 M HNO_3 (*b*) to a midrib of the Venus flytrap. (Online version in colour.)

of sensors and actuators in the Venus flytrap, which induces trap closing, locking and constricting in the same way as stimulation of its mechanosensors *in vivo*. The complete opening of a trap after the treatment of a midrib by hydrogen peroxide took 2 days, which is similar to experiments with LTP. Trap opening after HNO_3 treatment is slow and takes usually up to 3 days (figure 7). The complete opening of the trap during 2 days after mechanical stimulation includes two steps: opening the trap by moving the lobes and a slow transition from a concave to convex shape of the trap. If the trap caught a fly, it would remain closed for about a week for digestion before opening again [25].

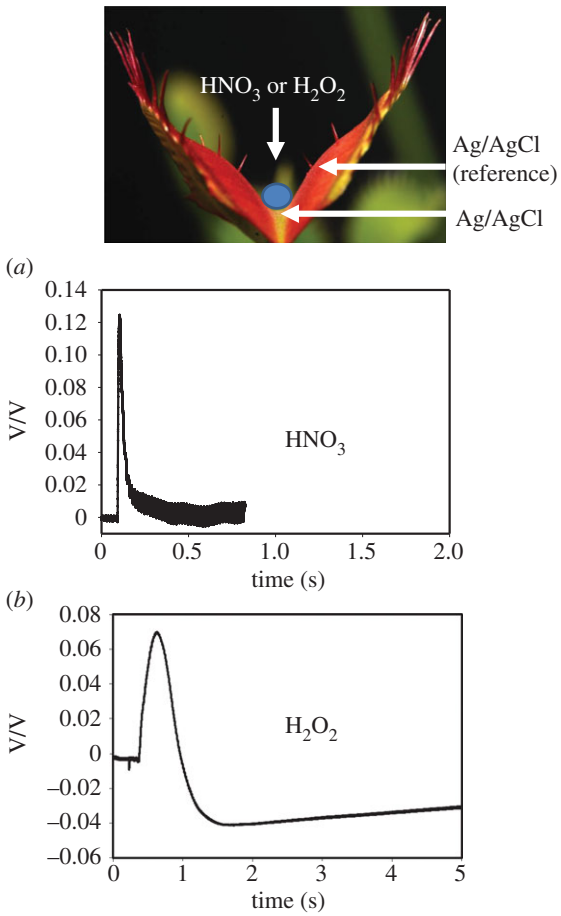

Figure 8. Potential difference between Ag/AgCl electrodes inserted in a lobe and midrib after deposition of a 10 µl drop of 0.01 M HNO_3 (*a*) or 3% H_2O_2 (*b*) on a midrib of the Venus flytrap. Measurements were performed at 100 000 scans s^{-1} with a low pass filter at 50 000 scans s^{-1}. All experimental results were reproduced at least 25 times using different plants. (Online version in colour.)

A drop of HNO_3 or H_2O_2 deposited on the midrib induces electrical signalling in the Venus flytrap (figure 8). Electrical signals, or action potentials, do not penetrate from the trap to a petiole. In some experiments, we measured single action potentials and sometimes multiple electrical signals after deposition of a small drop of HNO_3 or H_2O_2. Direct detection of the electrical signalling produced by plasma activation of plants was hindered by the measurement system capturing the strong electrical signals generated by the pulsed power system.

Control experiments were done to determine that UV light or neutral He or Ar gas flow did not induce morphing or closing the trap. The gas flow experiment used the same cold plasma jet device, but with the power system turned off. Thus, only the neutral gas exited the tube and impinged on the traps. The traps were held under the gas flow for 30 s and showed no motion of the traps. The UV test was done by placing the plant against the quartz tube during the plasma jet operation. The quartz tubes are transparent to UV, thus UV photons generated by argon and helium ions can pass through. Exposure to just the light emissions from the plasma in this fashion did not cause any change in the traps. With the fast recombination of charged particles beyond the jet, the remaining mechanism of the trap closing by plasma is the production of RONS compounds such as hydrogen peroxide.

The classical method of signal transduction analysis in plants and other organisms is specific inhibitory analysis of different components of signalling pathways such as ion channels, aquaporins and ion pumps. Blockers of ion channels and uncouplers inhibit electrical signal transduction in the Venus flytrap and the trap closing in response to mechanical stimuli of sensor hairs [29]. TEACl is known as a blocker of aquaporins [30] and K^+-channels [31] in plants. According to the literature, $HgCl_2$ is an efficient blocker of aquaporins [32]. Placing 10 µl of 10 mM TEACl or 1 mM $HgCl_2$ on the midrib of the trap 24 h before application of Ar or He plasma jet inhibits the trap closing for 20 s. Aqueous solutions of TEACl may affect the physiology of the plant because the Venus flytrap is notoriously sensitive to some ions [33]. Control plants were exposed to similar concentrations of KCl and $CaCl_2$ and they did not show inhibition of the trap closure. Usually, the concentration of salts in water from lakes and ponds is much higher and varies from 100 mg l^{-1} to 400 mg l^{-1} [34]. Water from lakes, ponds and rivers is the traditional source of water for the Venus flytrap in its natural habitat and *in vitro* [25].

4. Discussion

The plant electrical, chemical and mechanical pathways that are affected by cold plasma are discussed here. There are two major ways in which the cold plasma, in particular the plasma-generated RONS, interacts with the Venus flytrap. The first is via activation of phytoactuators to stimulate the closing mechanism. The second is via activation of ion channels to induce trap morphing from a convex to concave structure through osmotic water flow via aquaporins. A hydroelastic model for mechanical and plasma-induced closure is discussed to compare the behaviours of the closure process.

4.1. Phytosensors and phytoactuators

Plants have sophisticated nano- and micro-systems to sense environmental stimuli for adaptation and coordinated action. Consequently, plants generate various types of intracellular and intercellular electrical signals in response to these environmental stresses [17,24,25,35–37]. Detection and analysis of these signals in our experiment can provide insight into the physiological effects of cold plasma.

As living organisms, plants generate electrical signals, which propagate along different parts of the plant and can even be used for inter-plant communication [35,36]. Certain cells, such as nerve cells in animals and phloem cells in plants, possess excitable membranes through which electrical excitations can propagate in the form of action potentials. An action potential is a momentary change in electrical potential on the surface of a cell that takes place when the cell is stimulated. Initially, plants can respond to cold plasma at just the site of stimulation; however, excitation waves can be conducted via electrical signals along the cell plasma membranes throughout the entire plant, thereby affecting the whole plant. There are five major types of electrical signalling in plants: action, electrotonic, graded, receptor and streaming potentials. The action potential can propagate over the entire length of the cell membrane and along the conductive bundles of tissue with constant amplitude, duration and speed. Passive electrotonic potentials in plants exponentially decrease with distance. A graded potential is a wave of

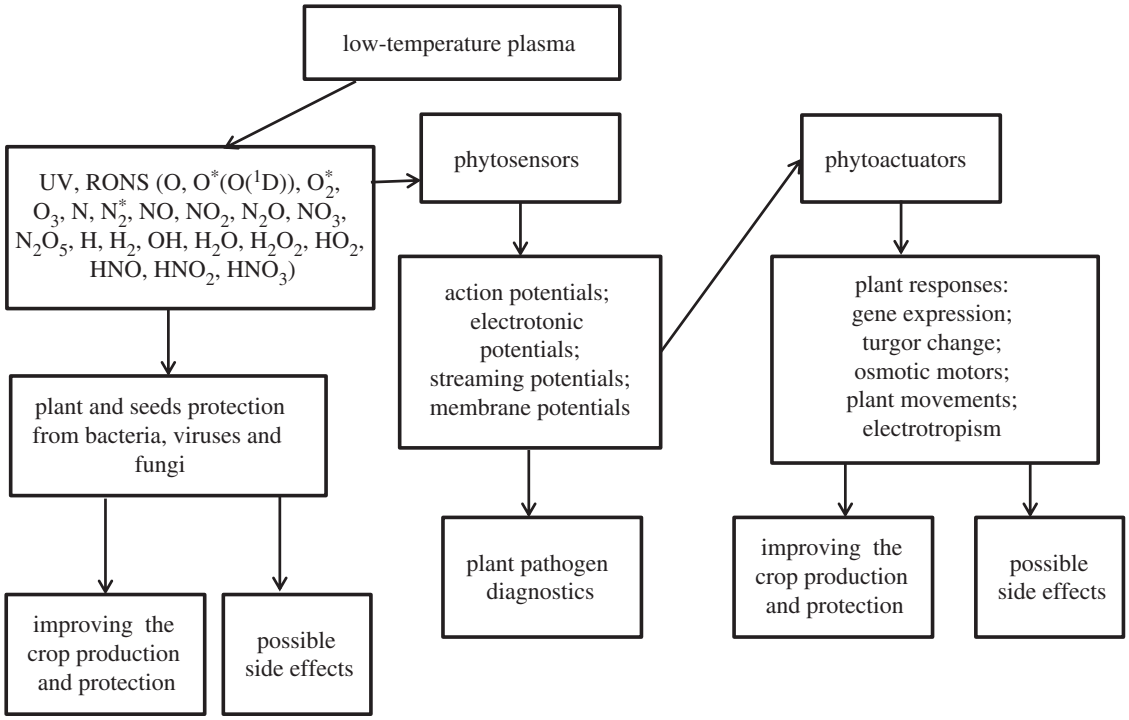

Figure 9. Schematic diagram of possible low-temperature plasma effects in seeds and plants.

electrical excitation that corresponds to the intensity of the stimulus. Receptor potentials are generated by mechanosensory ion channels. A streaming potential is a potential difference that arises across a capillary tube or membrane when a liquid is forced through it.

Electrochemical circuits control communication between phytosensors and phytoactuators in plants, trees, seeds and fruits. A phytosensor is a device that monitors the presence of different environmental stresses by detecting, recording and transmitting information related to a physiological process in a plant to phytoactuators. A phytoactuator is a part of a plant responsible for inducing or controlling specific plant response processes. Phytosensors, created by nature, are much more sensitive and efficient than man-made sensors. Memristors can be involved in electrochemical signal transduction between phytosensors and phytoactuators. Memristors are memory circuit elements whose properties depend on the history and state of the system. One such memristor can be a voltage-gated K^+ channel according to pharmaceutical analysis. Memristors can be involved in plant electrical memory.

Phytosensors potentially have tremendous utility as wide-area detectors for bio-surveillance of contamination by chemical or biological agents including plant pathogens. Plant responses can be considered in a few stages: (1) stimulus perception by a phytosensor, (2) electrochemical signal transmission, and (3) plant responses (figure 9).

Plants are ideal adaptive structures with smart sensing capabilities based on different types of tropisms. Plasma can induce different types of tropism such as chemotropism (RONS), electrotropism (electrical fields), thigmotropism (flow of gas) and phototropism (UV light). Our experiments and simulations narrowed the possible causes of the observed effects to chemotropism. We have confirmed that gas flow and UV radiation associated with the plasma are not the primary reasons for the observed effects [38]. The RONS produced by a cold plasma jet in atmospheric air appear to be the primary reason for plasma-induced activation of phytoactuators in plants, as proposed in figure 9. Some of these RONS are known to be signalling molecules, which control plants' developmental processes [13,14]. For example, nitric oxide is involved in the regulation of defence mechanisms in plant–pathogen interaction, promotion of the plant hypersensitive response, symbiosis, development of root hairs and control of stomatal opening.

4.2. The hydroelastic model

There are a few quantitative models that describe a possible mechanism of the Venus flytrap closing (for reviews, see [22,23,33]).To analyse the consecutive stages of the Venus flytrap closing and to elucidate the processes that govern these stages, we employed the recently developed hydroelastic curvature model [22]. The model is based on the assumption that the trap possesses curvature elasticity and consists of outer and inner hydraulic layers where different hydrostatic pressure can build up. The open state of the trap contains high elastic energy accumulation owing to the hydrostatic pressure difference between the outer and inner layers of the lobe. When stimulus-induced water flows from one hydraulic layer to another, the trap relaxes to the equilibrium configuration corresponding to the closed state. Water transport leads to extension of the cells on the exterior surface of the leaf and to a change in the natural curvature of the leaf, which probably drives the closure process.

The hydroelastic model includes bending elasticity, turgor pressure and water jets. The closure of the Venus flytrap represents non-muscular movement based on hydraulics and mechanical elasticity. The nastic movements in various plants involve a large internal pressure (turgor) that is actively regulated by the plants.

The leaf of the Venus flytrap is visualized as a thin, weakly curved elastic shell with principal natural curvatures that depend on the hydrostatic state of the two surface layers of cells A and B, where different hydrostatic pressures P_A and P_B are maintained. Two layers of cells, mechanically

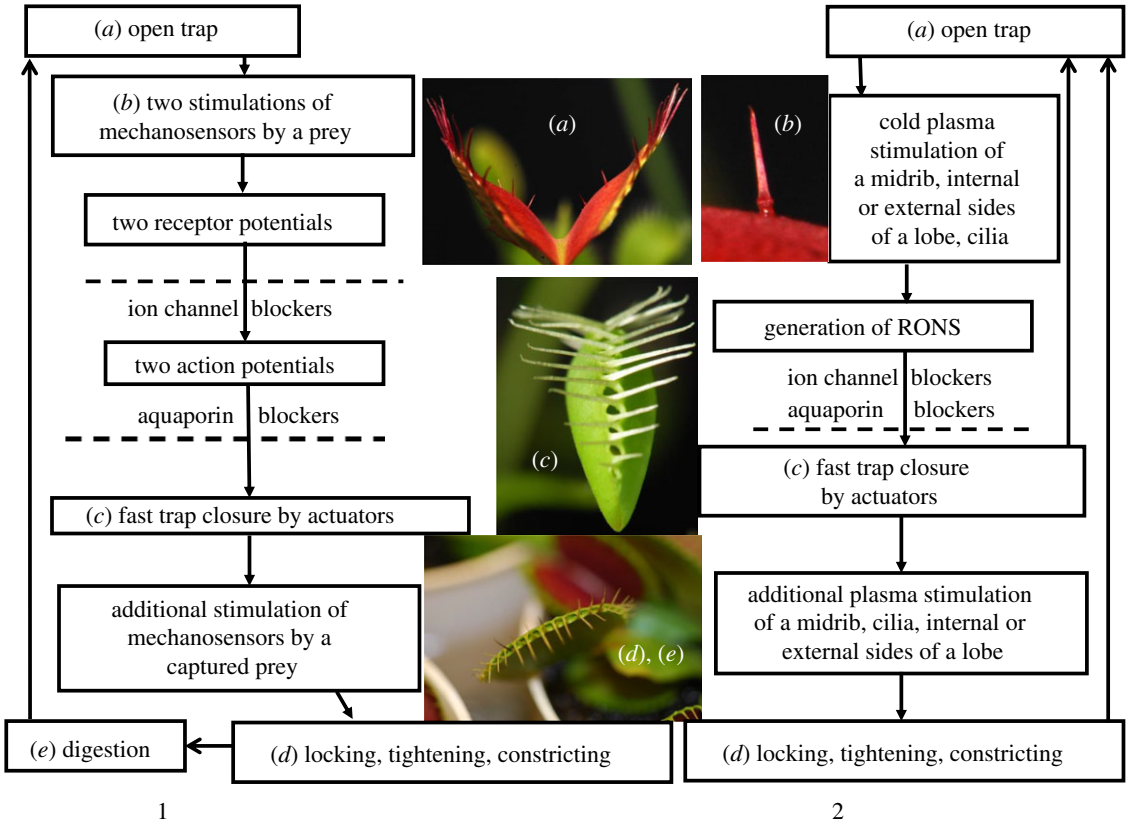

Figure 10. Mechanism of the Venus flytrap activation by mechanostimulation of trigger hairs (1) or by low-temperature plasma (2). Morphing structures in the Venus flytrap induced by mechanostimulation of trigger hairs (*b*) or by direct stimulation of the trap by low-temperature plasma: open trap (*a*); mechanosensitive trigger hair (*b*); closed trap (*c*); locked, tightened and constricted trap (*d*). (Online version in colour.)

connected to each other, behave like a bilayer couple where the in-plane expansion or contraction of any of them causes the change of curvature of the whole leaf. Unequal expansion of individual layers A and B results in bending of the leaf, and was described in terms of bending elasticity [22].

In the open state, the pressure in the upper layer is higher than that in the lower layer, maintaining the convex shape of the leaf. The fact that the hydrostatic pressure in different parts of the plant can be different is widely known [25,30,33]. This fast water redistribution is obviously driven by the pressure difference between different parts of the plant with different pressures, and exchange occurs through open pores.

The trigger signal causes fluid to rush from one layer to another. The leaf then relaxes to its equilibrium state corresponding to the closed configuration. The distance between the edges of the trap, d, was found [22] to vary with time as

$$d(t) = (1 - d_2)\ \exp\left\{\frac{\tau_a}{\tau_r}\left[1 - \exp\left(-\frac{t - t_s}{\tau_a}\right)\right] - \frac{(t - t_s)}{\tau_r}\right\} + d_2, \tag{4.1}$$

where $d(t)$ is the normalized distance between the edges of the trap; τ_a is the characteristic time of the opening kinetics; τ_r is the characteristic time of fluid transfer; t is the time; t_s is the moment when the trigger reaches threshold value; and d_2 is the final relative distance between the edges of two lobes in the closed state. Both distance and mean curvature of the leaf are described by the same function of time. The mean curvature changes from a positive to a negative value during the process of trap closure, while the Gaussian curvature stays positive; it decreases in the beginning, reaches zero, and then begins to increase. The hydroelastic curvature model predicts the kinetics of consecutive stages of the trap closure. This gives us the opportunity to justify the basic assumption of the hydroelastic curvature model and to determine the variation of kinetic parameters of the Venus flytrap closure (figures 5 and 6). The speed v of trap closure can be obtained from equation (4.1) as follows:

$$v(t) = \frac{(1 - d_2)}{\tau_w}\ \exp\left\{\frac{\tau_{\text{pore}}}{\tau_w}\left[1 - \exp\left(-\frac{t - t_{th}}{\tau_{\text{pore}}}\right)\right] - \frac{(t - t_{th})}{\tau_w}\right\}$$
$$\left[\exp\left(-\frac{t - t_{th}}{\tau_{\text{pore}}}\right) - 1\right]. \tag{4.2}$$

4.3. Reactive oxygen and nitrogen species and mechanisms of the trap morphing and closing

RONS are involved in signal transduction, interactions with ion channels and cell death. The specific biological response of a plant to RONS depends on the chemical identity of the RONS, the intensity of the signal, sites of production, the plant developmental stage, previous stresses encountered and interactions with other signalling molecules such as nitric oxide, lipid messengers and plant hormones. The most important ROS radicals include superoxide, hydroxyl, hydroperoxyl, hydrogen peroxide, alkoxy, peroxy and singlet oxygen. These species are cytotoxic to plants and can lead to cell death. For example, the reaction of nitric oxide with the superoxide radical produces a short-lived oxidant peroxynitrile, which is a potent inducer of cell death.

Figure 10 shows a comparison of the proposed mechanism of closure of the Venus flytrap by mechanical stimulation of trigger hairs (1) [17,24,25] and by cold plasma (2). The closing

process essentially involves a change in the leaf's geometry. The upper leaf is convex in the open state and concave in its closed position. Trap closure is believed to represent non-muscular movement based on hydraulics and mechanics [22,39]. The nastic movement in various plants involves a large internal pressure (turgor). It is quite likely that these movements are driven by differential turgor that is actively regulated by the plants. Trap closure occurs via quick changes in the curvature of each lobe rather than by movement of the leaf as a whole. These anatomical features were selected as the basis of the hydroelastic curvature model (equations (4.1) and (4.2)).

The mechanism of the fast trap closing (figure 10) induced by cold plasma consists of a few stages:

(i) Generation of RONS (figure 3) is due to air interaction with the plasma jet; (figure 3).
(ii) RONS activate voltage-gated ion channels and transmission of action potentials (figure 8).
(iii) Transport of ions induces opening of aquaporins as water jets. Fast water transport induces redistribution of water in the trap.
(iv) Redistribution of water pressure in the trap leads to its fast closing and morphing according to equations (4.1) and (4.2). Theoretical treatment coincides with experimental data (figures 5 and 6). The driving force of the closing process is most probably the elastic curvature energy stored and locked in the leaves because of a pressure difference between the upper and lower layers of the leaf [22]. The open state of the trap contains high elastic energy accumulated as a result of the hydrostatic pressure difference between the hydraulic layers of the lobe. The trigger signal opens the water pores between these layers and the fluid transfers from the upper to the lower layer. The leaf relaxes to its equilibrium state, corresponding to the closed configuration.

While we hypothesize that RONS, which have been previously observed and confirmed to be present in atmospheric-pressure plasma jets, are responsible for the observed effects, direct measurements of the RONS concentration or reliable computer simulations of our specific plasma composition is needed and could be a subject of further work. The measurement of atmospheric plasma-produced RONS has been done by other researchers for different plasma source designs [40]. The main RONS species of interest have been O, O_3, OH, N and NO. Knake *et al*. [41] used two-photon laser-induced fluorescence (TALIF) to measure the density of atomic oxygen in an RF atmospheric plasma jet with varying amounts of O_2 added. Reuter *et al*. [42] used optical emissions spectroscopy to measure the concentration of atomic oxygen in a high-voltage AC plasma jet using argon as the main gas but with a shielding gas of either N_2 or O_2 [42]. Singlet delta oxygen molecules have also been measured by infrared emission spectroscopy [43]. Many researchers have used laser-induced fluorescence (LIF) to measure OH and/or atomic oxygen densities in RF [44,45] or pulsed DC plasma jets [46]. Atomic nitrogen density has been measured using TALIF in RF plasma jets [47] and a pulsed corona [48]. Ozone density has been measured with UV absorption spectroscopy for RF plasma jets [49,50]. Finally, NO species have been measured in RF plasma jets with mass spectrometry [51], laser absorption spectroscopy [52] and LIF [53]. The pulsed DC plasma jets would most closely resemble the source used in this work. RF-powered jets typically output more current and power than pulsed DC jets, which alters the plasma chemistry. However, the behaviour of atmospheric plasma jets depends on the geometry as well as the ambient environment, so much that results cannot be taken as parallels, though general trends may be similar.

Modelling and simulations of plasma jets involve solutions of rather complex multi-physics problems [54]. Although the plasma plume appears steady, it consists of guided ionization waves travelling along the jet channel at speeds that are orders of magnitude faster than the gas flow velocity. A complete and detailed simulation of the plasma would need to include gas breakdown, plasma formation, propagation of the ionization waves, electron-driven chemistry of noble gas plasma, noble gas–air mixing and an affluent region outside the plasma plume where long-lived active species are mixed with ambient gas [55]. Such a model would require taking into account electrons, ions, many neutral species such as O, O*(O(1D)), O^2–O_3, N, N_2*, NO, NO_2, N_2O, N_2O_5, H, H_2, OH, H_2O, H_2O_2, HO_2, HNO, HNO_2, HNO_3 and hundreds of chemical reactions [56,57]. As a result, simulations or plasma jets so far have been performed only with simplified chemistries [58,59] or with global plasma models [60,61]. However, such a complete model is desirable because understanding plasma control of plant morphing could extend the research beyond biology and help design adaptive structures and bioinspired intelligent materials.

5. Conclusion

We have observed for the first time that the *D. muscipula* Ellis can be activated by LTP without direct touching of the plant by plasma. Helium, helium + air and argon plasma jets induced fast movements and morphing of the Venus flytrap similar to the stimulation of mechanosensors or trigger hairs *in vivo*. By evaluating possible contributions of different plasma components to plant activation, we have concluded that plasma-generated RONS must be primarily responsible for trap closing, locking, tightening, and its transition from convex to concave. Control experiments showed that UV light or He or Ar gas flow did not induce morphing or closing the trap. Direct experiments have confirmed that 10 µl drops of H_2O_2 or HNO_3 (common RONS in biosystems) on the midrib can induce closing of the Venus flytrap similar to that induced by the cold plasma. The morphing behaviour of the Venus flytrap involves processes associated with activation of ion channels and water jets (aquaporins) in these plants. We argue that plasma induces the trap closing by producing RONS near the trap surface. We have measured action potentials induced by liquid drops of H_2O_2 or HNO_3 and attempted to measure electrical signalling during plasma activation of the plants. The latter turned out to be challenging. We have observed that plant tissue works as an antenna and collects electrical noise generated by the plasma power system. This noise makes direct measurement of plant electrical signals during plasma activation more complicated. We plan to further study these effects in future work.

Data accessibility. The data that support the findings of this study are available from the corresponding author, Alexander G. Volkov, upon reasonable request.

Authors' contributions. A.G.V., K.G.X. and V.I.K. designed and performed experiments. All authors recorded and evaluated responses of plants to cold plasma activation. All authors wrote the manuscript. All authors read and approved the manuscript.

Competing interests. The authors have no financial or personal relationships with other people or organizations that might inappropriately influence or bias the work.

Funding. This work was supported by the National Science Foundation (grant EPSCoR RII-Track-1 Cooperative Agreement OIA-1655280).

References

1. Lemström S. 1904 *Electricity in agriculture and horticulture*. London, UK: The Electrician Printing & Publishing Company, Limited.
2. Murr LE. 1963 Plant growth response in a simulated electric field-environment. *Nature* **200**, 490–491. (doi:10.1038/200490b0)
3. Ito M, Ohta T, Hori M. 2012 Plasma agriculture. *J. Korean Phys. Soc.* **60**, 937–943. (doi:10.3938/jkps.60.937)
4. Pankaj SK. 2018 Effects of cold plasma on food quality: a review. *Foods* **7**, 4. (doi:10.3390/foods7010004)
5. Bourke P, Ziuzina D, Boehm D, Cullen PJ, Keener K. 2018 The potential of cold plasma for safe and sustainable food production. *Trends Biotechnol.* **36**, 615–626. (doi:10.1016/j.tibtech.2017.11.001)
6. Machala Z, Pavlovich MJ. 2018 A new phase in applied biology. *Trends Biotechnol.* **36**, 577–578. (doi:10.1016/j.tibtech.2018.04.001)
7. Laroussi M, Keidar M, Hori M. 2018 Special issue on plasma medicine. *Plasma* **1**, 259–260. (doi:10.3390/plasma1020022)
8. Graves DB, Bauer G. 2018 Key roles of reactive oxygen and nitrogen species. In *Comprehensive clinical plasma medicine* (eds H-R Metelmann, T von Woedtke, K-D Weltmann), pp. 71–82. Cham, Switzerland: Springer International Publishing.
9. Mittler R. 2017 ROS are good. *Trends Plant Sci.* **22**, 11–19. (doi:10.1016/j.tplants.2016.08.002)
10. Tian W, Kushner MJ. 2014 Atmospheric pressure dielectric barrier discharges interacting with liquid covered tissue. *J. Phys. D Appl. Phys.* **47**, 165201. (doi:10.1088/0022-3727/47/16/165201)
11. Chen C, Liu DX, Liu ZC, Yang AJ, Chen HL, Shama G, Kong MG. 2014 A model of plasma-biofilm and plasma-tissue interactions at ambient pressure. *Plasma Chem. Plasma Process.* **34**, 403–441. (doi:10.1007/s11090-014-9545-1)
12. Misra NN, Schlüter O, Cullen PJ. 2016 *Cold plasma in food and agriculture: fundamentals and applications*. Amsterdam, The Netherlands: Elsevier.
13. Lu X, Naidis GV, Laroussi M, Reuter S, Graves DB, Ostrikov K. 2016 Reactive species in non-equilibrium atmospheric-pressure plasmas: generation, transport, and biological effects. *Phys. Rep.* **630**, 1–84. (doi:10.1016/j.physrep.2016.03.003)
14. Demidchik V. 2003 Free oxygen radicals regulate plasma membrane Ca^{2+}- and K^{+}-permeable channels in plant root cells. *J. Cell Sci.* **116**, 81–88. (doi:10.1242/jcs.00201)
15. Darwin C. 1880 *The power of movement in plants*. London, UK: Murray.
16. Jacobson SL. 1965 Receptor response in Venus's flytrap. *J. Gen. Physiol.* **49**, 117–129. (doi:10.1085/jgp.49.1.117)
17. Volkov AG, Adesina T, Jovanov E. 2008 Charge induced closing of *Dionaea muscipula* Ellis trap. *Bioelectrochemistry* **74**, 16–21. (doi:10.1016/j.bioelechem.2008.02.004)
18. Lloyd FE. 1940 *The carnivorous plants*. Waltham, MA: Chronica Botanica Co.
19. Hodick D, Sievers A. 1989 On the mechanism of trap closure of Venus flytrap (*Dionaea muscipula* Ellis). *Planta* **179**, 32–42. (doi:10.1007/BF00395768)
20. Williams SE, Bennett AB. 1982 Leaf closure in the Venus flytrap: an acid growth response. *Science* **218**, 1120–1122. (doi:10.1126/science.218.4577.1120)
21. Forterre Y, Skotheim JM, Dumals J, Mahadevan L. 2005 How the Venus flytrap snaps. *Nature* **433**, 421–425. (doi:10.1038/nature03185)
22. Markin VS, Volkov AG, Jovanov E. 2008 Active movements in plants: mechanism of trap closure by *Dionaea muscipula* Ellis. *Plant Signal. Behav.* **3**, 778–783. (doi:10.4161/psb.3.10.6041)
23. Yang R, Lenaghan SC, Li Y, Oi S, Zhang M. 2012 Mathematical modeling, dynamics analysis and control of carnivorous plants. In *Plant electrophysiology* (ed. AG Volkov), pp. 63–83. Berlin, Germany: Springer.
24. Volkov AG, Adesina T, Markin VS, Jovanov E. 2008 Kinetics and mechanism of *Dionaea muscipula* trap closing. *Plant Physiol.* **146**, 694–702. (doi:10.1104/pp.107.108241)
25. Volkov AG, Pinnock M-R, Lowe DC, Gay MS, Markin VS. 2011 Complete hunting cycle of *Dionaea muscipula*: consecutive steps and their electrical properties. *J. Plant Physiol.* **168**, 109–120. (doi:10.1016/j.jplph.2010.06.007)
26. van Gessel AFH, Carbone EAD, Bruggeman PJ, van der Mullen JJAM. 2012 Laser scattering on an atmospheric pressure plasma jet: disentangling Rayleigh, Raman and Thomson scattering. *Plasma Sources Sci. Technol.* **21**, 015003. (doi:10.1088/0963-0252/21/1/015003)
27. Xu KG, Doyle SJ. 2016 Measurement of atmospheric pressure microplasma jet with Langmuir probes measurement of atmospheric pressure microplasma jet with Langmuir probes. *J. Vac. Sci. Technol. A* **34**, 051301. (doi:10.1116/1.4959565)
28. Köhler B, Hills A, Blatt MR. 2003 Control of guard cell ion channels by hydrogen peroxide and abscisic acid indicates their action through alternate signaling pathways. *Plant Physiol.* **131**, 385–388. (doi:10.1104/pp.016014)
29. Volkov AG, Coopwood KJ, Markin VS. 2008 Inhibition of the *Dionaea muscipula* Ellis trap closure by ion and water channels blockers and uncouplers. *Plant Sci.* **175**, 642–649. (doi:10.1016/j.plantsci.2008.06.016)
30. Tyerman SD, Niemietz CM, Bramley H. 2002 Plant aquaporins: multifunctional water and solute channels with expanding roles. *Plant Cell Environ.* **25**, 173–194. (doi:10.1046/j.0016-8025.2001.00791.x)
31. Krol E, Dziubinska H, Stolarz M, Trebacz K. 2006 Effects of ion channel inhibitors on cold- and electrically-induced action potentials in *Dionaea muscipula*. *Biol. Plant.* **50**, 411–416. (doi:10.1007/s10535-006-0058-5)
32. Savage DF, Stroud RM. 2007 Structural basis of aquaporin inhibition by mercury. *J. Mol. Biol.* **368**, 607–617. (doi:10.1016/j.jmb.2007.02.070)
33. Poppinga S, Bauer U, Speck T, Volkov AG. 2017 Motile traps. In *Carnivorous plants: physiology, ecology, and evolution*. Oxford, UK: Oxford University Press.
34. Drever JI. 1997 *The geochemistry of natural waters: surface and groundwater environments*, 3rd edn. Englewood Cliffs, NJ: Prentice Hall.
35. Volkov AG, Shtessel YB. 2018 Electrical signal propagation within and between tomato plants. *Bioelectrochemistry* **124**, 195–205. (doi:10.1016/j.bioelechem.2018.08.001)
36. Volkov AG, Shtessel YB. 2017 Electrotonic signal transduction between Aloe vera plants using underground pathways in soil: experimental and analytical study. *AIMS Biophys.* **4**, 576–595. (doi:10.3934/biophy.2017.4.576)
37. Hedrich R, Neher E. 2018 Venus flytrap: how an excitable, carnivorous plant works. *Trends Plant Sci.* **23**, 220–234. (doi:10.1016/j.tplants.2017.12.004)
38. Volkov AG, Xu KG, Kolobov VI. 2017 Cold plasma interactions with plants: morphing and movements of Venus flytrap and Mimosa pudica induced by argon plasma jet. *Bioelectrochemistry* **118**, 100–105. (doi:10.1016/j.bioelechem.2017.07.011)
39. Guo Q, Dai E, Han X, Xie S, Chao E, Chen Z. 2015 Fast nastic motion of plants and bioinspired

structures. *J. R. Soc. Interface* **12**, 20150598. (doi:10.1098/rsif.2015.0598)

40. Ono R. 2016 Optical diagnostics of reactive species in atmospheric-pressure nonthermal plasma. *J. Phys. D Appl. Phys.* **49**, 083001. (doi:10.1088/0022-3727/49/8/083001)
41. Knake N, Reuter S, Niemi K, Schulz-von der Gathen V, Winter J. 2008 Absolute atomic oxygen density distributions in the effluent of a microscale atmospheric pressure plasma jet. *J. Phys. D Appl. Phys.* **41**, 194006. (doi:10.1088/0022-3727/41/19/194006)
42. Reuter S, Tresp H, Wende K, Hammer MU, Winter J, Masur K, Schmidt-Bleker A, Weltmann KD. 2012 From RONS to ROS: tailoring plasma jet treatment of skin cells. *IEEE Trans. Plasma Sci.* **40**, 2986–2993. (doi:10.1109/TPS.2012.2207130)
43. Sousa JS, Niemi K, Cox LJ, Algwari QT, Gans T, O'Connell D. 2011 Cold atmospheric pressure plasma jets as sources of singlet delta oxygen for biomedical applications. *J. Appl. Phys.* **109**, 123302. (doi:10.1063/1.3601347)
44. Voráč J, Obrusník A, Procházka V, Dvořák P, Talába M. 2016 Corrigendum: spatially resolved measurement of hydroxyl radical (OH) concentration in argon RF plasma jet by planar laser-induced fluorescence (2014 Plasma Sources Sci. Technol. 23 025011). *Plasma Sources Sci. Technol.* **25**, 059502. (doi:10.1088/0963-0252/25/5/059502)
45. Verreycken T, Mensink R, Van Der Horst R, Sadeghi N, Bruggeman PJ. 2013 Absolute OH density measurements in the effluent of a cold atmospheric-pressure Ar-H_2O RF plasma jet in air. *Plasma Sci. Technol.* **22,** 055014. (doi:10.1088/0963-0252/22/5/055014)
46. Yonemori S, Ono R. 2014 Flux of OH and O radicals onto a surface by an atmospheric-pressure helium plasma jet measured by laser-induced fluorescence. *J. Phys. D Appl. Phys.* **47,** 125401. (doi:10.1088/0022-3727/47/12/125401)
47. Wagenaars E, Gans T, O'Connell D, Niemi K. 2012 Two-photon absorption laser-induced fluorescence measurements of atomic nitrogen in a radio-frequency atmospheric-pressure plasma jet. *Plasma Sources Sci. Technol.* **21,** 042002. (doi:10.1088/0963-0252/21/4/042002)
48. Ono R, Teramoto Y, Oda T. 2009 Measurement of atomic nitrogen in N_2 pulsed positive corona discharge using two-photon absorption laser-induced fluorescence. *Jpn. J. Appl. Phys.* **48**, 2–5. (doi:10.1143/JJAP.48.122302)
49. Schulz-Von Der Gathen V, Buck V, Gans T, Knake N, Niemi K, Reuter S, Schaper L, Winter J. 2007 Optical diagnostics of micro discharge jets. *Contrib. Plasma Phys.* **47**, 510–519. (doi:10.1002/ctpp.200710066)
50. Zhang S, Van Gaens W, Van Gessel B, Hofmann S, Van Veldhuizen E, Bogaerts A, Bruggeman P. 2013 Spatially resolved ozone densities and gas temperatures in a time modulated RF driven atmospheric pressure plasma jet: an analysis of the production and destruction mechanisms. *J. Phys. D Appl. Phys.* **46,** 205202. (doi:10.1088/0022-3727/46/20/205202)
51. Stoffels E, Gonzalvo YA, Whitmore TD, Seymour DL, Rees JA. 2006 A plasma needle generates nitric oxide. *Plasma Sources Sci. Technol.* **15**, 501–506. (doi:10.1088/0963-0252/15/3/028)
52. Pipa AV, Reuter S, Foest R, Weltmann KD. 2012 Controlling the NO production of an atmospheric pressure plasma jet. *J. Phys. D Appl. Phys.* **45,** 085201. (doi:10.1088/0022-3727/45/8/085201)
53. Van Gessel AFH, Alards KMJ, Bruggeman PJ. 2013 NO production in an RF plasma jet at atmospheric pressure. *J. Phys. D Appl. Phys.* **46,** 265202. (doi:10.1088/0022-3727/46/26/265202)
54. Babaeva NY, Naidis GV. 2018 Modeling of plasmas for biomedicine. *Trends Biotechnol.* **36**, 603–614. (doi:10.1016/j.tibtech.2017.06.017)
55. Darny T, Pouvesle J-M, Fontane J, Joly L, Dozias S, Robert E. 2017 Plasma action on helium flow in cold atmospheric pressure plasma jet experiments. *Plasma Sources Sci. Technol.* **26**, 105001. (doi:10.1088/1361-6595/aa8877)
56. Schmidt-Bleker A, Winter J, Bösel A, Reuter S, Weltmann KD. 2015 On the plasma chemistry of a cold atmospheric argon plasma jet with shielding gas device. *Plasma Sources Sci. Technol.* **25**, 015005. (doi:10.1088/0963-0252/25/1/015005)
57. Lietz AM, Kushner MJ. 2018 Molecular admixtures and impurities in atmospheric pressure plasma jets. *J. Appl. Phys.* **124**, 153303. (doi:10.1063/1.5049430)
58. Boeuf JP, Yang LL, Pitchford LC. 2013 Dynamics of a guided streamer ('plasma bullet') in a helium jet in air at atmospheric pressure. *J. Phys. D Appl. Phys.* **46**, 015201. (doi:10.1088/0022-3727/46/1/015201)
59. Breden D, Raja LL. 2014 Computational study of the interaction of cold atmospheric helium plasma jets with surfaces. *Plasma Sources Sci. Technol.* **23**, 065020. (doi:10.1088/0963-0252/23/6/065020)
60. Gaens WV, Iseni S, Schmidt-Bleker A, Weltmann KD, Reuter S, Bogaerts A. 2015 Numerical analysis of the effect of nitrogen and oxygen admixtures on the chemistry of an argon plasma jet operating at atmospheric pressure. *New J. Phys.* **17**, 033003. (doi:10.1088/1367-2630/17/3/033003)
61. Schröter S *et al.* 2018 Chemical kinetics in an atmospheric pressure helium plasma containing humidity. *Phys. Chem. Chem. Phys.* **20**, 24 263–24 286. (doi:10.1039/C8CP02473A)